Engineering Geology 163 (2013) 11–19

Contents lists available at ScienceDirect

Engineering Geology

journal homepage: www.elsevier.com/locate/enggeo

Evaluation of rock anisotropy using 3D X-ray computed tomography

Tae Sup Yun [a], Yeon Jong Jeong [a], Kwang Yeom Kim [b,*], Ki-Bok Min [c]

[a] School of Civil and Environmental Engineering, Yonsei University, Yonsei-ro 50, Seodaemun-gu, Seoul 120-749, Republic of Korea
[b] Korea Institute of Construction Technology, 283 Goyangdae-ro, Ilsanseo-gu, Goyang 411-712, Republic of Korea
[c] Department of Energy Resources Engineering, Seoul National University, Gwanak-ro 599, Gwanak-gu, Seoul 151-744, Republic of Korea

ARTICLE INFO

Article history:
Received 6 October 2012
Received in revised form 22 May 2013
Accepted 26 May 2013
Available online 11 June 2013

Keywords:
Rock fabric
Anisotropy
X-ray computed tomography
Statistics
Clustering

ABSTRACT

The anisotropic nature of fabric and internal structures plays a significant role in fluid flow, heat transfer, and geomechanical behavior in rock. The existence and orientation of anisotropy in various rocks have been evaluated using laboratory experiments and image analyses to characterize anisotropic pore networks, microfractures, mineralogy, grain fabric, and stiffness from micro- to macro-scales. We present an assessment of anisotropy in rock by systematic and planar clustering of three-dimensional X-ray attenuation values and associated statistical analysis on the basis that X-ray CT numbers directly represent the internal density of the mineral fabric in the rock mass. Variation in voxel values across the slicing plane for a given orientation enables identification of the unique orientation of anisotropy in rock. The proposed concept is validated using a 3D virtual structure and is applied to four different rock types. The sensitivity of anisotropic features and the image noise effect are further explored to highlight the robustness of the proposed method for evaluating the anisotropy of rock fabrics.

1. Introduction

Anisotropy in rocks originates from stratification, metamorphic foliation, and discontinuities, and grain fabrics affect the mechanical, thermal, hydraulic, and seismic behaviors of rock (Johnston and Christensen, 1995; Amadei, 1996). The significance of such anisotropy has been emphasized in studies of in situ stress (Adamei and Goodman, 1982), fracture propagation (Timms et al., 2010; Ajibade et al., 2012), and anisotropic fluid flow and heat transfer (Deming, 1994; Davis et al., 2007). It is also critical to determine the anisotropic parameters and symmetry plane in rocks in resolving the constitutive relations, which is a long-standing issue.

Anisotropic rock can be classified into two classes depending on the apparent visibility of anisotropy (Barla, 1974): class A includes rocks with anisotropic properties that may appear isotropic, and class B includes rocks with visible evidence of anisotropy. The symmetry plane in class B rocks (e.g., shale, gneiss, schist) is readily observable and is well matched with experimentally derived properties (Cho et al., 2012; Kim et al., 2012a), whereas in class A rocks (e.g., granite and sandstone) additional effort is required to identify the symmetry planes. Most methods of characterizing anisotropic rock require a priori knowledge of the symmetry plane through visible observations. It is therefore challenging to characterize anisotropy when it is not visually apparent.

Three-dimensional (3D) X-ray computed tomography (CT) enables the internal microstructures in a rock mass to be visualized. In studies of anisotropy, this technique has been applied to pore networks, fabrics, crack propagation, and the elastic modulus, using image-based characterization and stochastic simulations, which are commonly corroborated by systematic experiments and numerical investigations (Scholz and Koczynski, 1979; Pros et al., 1998; Inglis and Pietruszczak, 2003; Ketcham, 2005; Ketcham and Iturrino, 2005; Nakashima et al., 2008; Arad et al., 2010; Timms et al., 2010; Nasseri et al., 2011). These approaches generally involve the pre-processing of images to segment existing phases, and are applicable to a wide range of rock specimens, including volcanic rock, schist, granite, dolomite, marine sediment, and sandstone (Sun and Kodawa, 1992; Ruiz de Argandoda et al., 1999; Lindquist and Venkatarangan, 2000; Ketcham, 2005; Ketcham and Iturrino, 2005; Nasseri et al., 2011; Cnudde et al., 2011a). The petrophysical properties of construction materials have also been widely characterized using X-ray CT and associated image analysis techniques (Cnudde et al., 2011b; Lanzon et al., 2012; Yun et al., 2012). Although the specimen size for X-ray CT analyses should be less than a couple of centimeters, the anisotropy of resistivity, magnetic susceptibility, seismicity, and rock strength can also be evaluated in terms of grain shape, crystalline structure, and fractures to improve our fundamental understanding of the relation between anisotropy and the dominant properties of the rock mass (Uyeda et al., 1963; Gergoire et al., 1998; Luneburg et al., 1999; Zeng et al., 2008; Ben and Onwuemesi, 2009; Ajibade et al., 2012).

Because the X-ray attenuation values in reconstructed CT images depend on the internal density of the mineral fabric and the atomic weights of the elements in minerals, a particular clustering of 3D

* Corresponding author. Tel.: +82 31 910 0225; fax: +82 31 910 0211.
E-mail addresses: taesup@yonsei.ac.kr (T.S. Yun), jyjrafael@yonsei.ac.kr (Y.J. Jeong), kimky@kict.re.kr (K.Y. Kim), kbmin@snu.ac.kr (K.-B. Min).

0013-7952/$ – see front matter © 2013 Elsevier B.V. All rights reserved.
http://dx.doi.org/10.1016/j.enggeo.2013.05.017

attenuation values can indicate the existence of anisotropy and its orientation. Here, we propose a novel method of determining the nature of anisotropy in rocks using 3D X-ray CT, based on the notion that anisotropy in a rock mass can be identified by the spatial distribution of attenuation values crossed by systematically oriented slicing planes, followed by statistical evaluation of variations in the form of planar clustering. The proposed method is applicable regardless of the visibility of the anisotropy or the origin of the symmetry plane, and utilizes the original X-ray attenuation values without any pre-processing of images. Here, we present and validate the proposed method, and discuss its application to samples of four different types of rock.

2. Evaluation of anisotropy using a slicing plane

2.1. Validation of the proposed concept

X-ray attenuation value of every CT voxel is related to density of rock (solid and pores) and atomic weight of the elements comprised in that voxel. Any anomalous or heterogeneous internal structure within a rock specimen therefore exhibits uniquely clustered attenuation values. For layered structures, the clustering of similar attenuation values may define a planar geometry with a specific orientation, and should periodically alternate in the direction normal to the plane of the structure. Therefore, we propose the following steps for evaluating anisotropy in rock.

The voxel structure of the rock specimen is assumed to have a size of $D \times D \times D$ on 3D X-ray CT imaging. The slicing plane P defined at the center of the 3D voxel structure and the corresponding normal vector line L are rotated together with a trend θ (the clockwise angle between a linear feature and the north direction) and a plunge ϕ (the acute angle between a linear feature and a horizontal line). Let the group of attenuation values crossed by the slicing plane for a given orientation be G, and the computed sliced area be A^G and the mean be μ^G. The slicing plane P moves sequentially along the normal vector line L, which is discretized with m number of points with equal spacing. Note that the maximum length of the normal vector line L is defined as $\sqrt{3}D$ (e.g., the diagonal length of 3D voxel data). The orientation of the slicing plane P changes every 1° from $\theta = 0°$ to 360° and from $\phi = 0°$ to 90° for the trend and plunge, respectively, to systematically scan the entire volume of the 3D voxel structure. Then, it is possible to obtain the mean of sliced voxels $\mu^G_{m,\phi\theta}$ and the area $A^G_{m,\phi\theta}$ for all the possible sets of trend and plunge. Fig. 1 schematically shows the 3D image data sliced by the plane P with the corresponding normal vector line L.

When the slicing plane P is oriented parallel to the alternating layers with the normal vector at θ_p and ϕ_p, the standard deviation of μ^G_m (i.e., the mean values along the normal vector line for a given orientation) is supposed to be highest. In contrast, when the normal vectors of slicing planes begin deviating from θ_p and ϕ_p, the magnitude of the variation in μ^G_m will decrease. Therefore, it is feasible to assess the orientation of anisotropic layers by mapping σ^{μ^G} (i.e., the standard deviation of μ^G_m) for entire ranges of trend and plunge. As the sliced area A^G varies along the normal vector line, the weighted standard deviation $\sigma^{\mu^G}_w$ is computed.

The proposed method for assessing the presence and orientation of anisotropic structures is validated by an analysis of 3D virtual structures in which periodically alternating layers are purposely imposed. The 3D voxel domain of 251 × 251 × 251 voxels, as a base, is constructed and initially filled with normally distributed random numbers having a mean of 1500 and standard deviation of 100. Layers with normally distributed random numbers having a mean of 2500 and standard deviation of 100 are periodically inserted with a thickness of 5 voxels, spacing of 30 voxels, and trend and plunge of 240° and 60°, respectively, as shown by Case 1 in Fig. 2a. A second simulated case includes an additional layer, with a trend and plunge of 150° and 30°, respectively (Case 2, Fig. 2b), which enables observation of the effect of crossed layers. Following the prescribed procedures, the weighted standard deviation $\sigma^{\mu^G}_w$ and the weighted mean $\mu^{\mu^G}_w$ are obtained for all possible sets of trend and plunge. Fig. 3a and b shows the coefficient of variation $\left(c_v = \sigma^{\mu^G}_w / \mu^{\mu^G}_w\right)$ values for Cases 1 and 2 plotted on an equal-angle lower-hemisphere stereonet. The prescribed orientation of virtual layers shows a good match with the direction of the highest c_v observed. The yellow great circles indicate the slicing plane at the corresponding highest c_v. As the slicing plane deviates from the orientation of the layered structure, the coefficient of variation shows a sharp decrease. The profiles of mean values, μ^G_m, when the slicing plane is parallel to the synthetic layers (i.e., orientation of highest c_v) are presented in Fig. 3c and d. Because in Case 1, the layers periodically exist, the mean values oscillate between 2500 and 1500. In Case 2, the mean layer value of 2500 remains and a mean >1600 appears because of the existence of the second layer. The probability distribution at points A (layer) and B (zone between layers) exactly reflects the group of imposed random values (Fig. 3e and f). Therefore, we propose that this procedure would enable identification of the orientation of anisotropic structure solely on the basis of the systematic clustering of attenuation values and spatial analysis of variations in G.

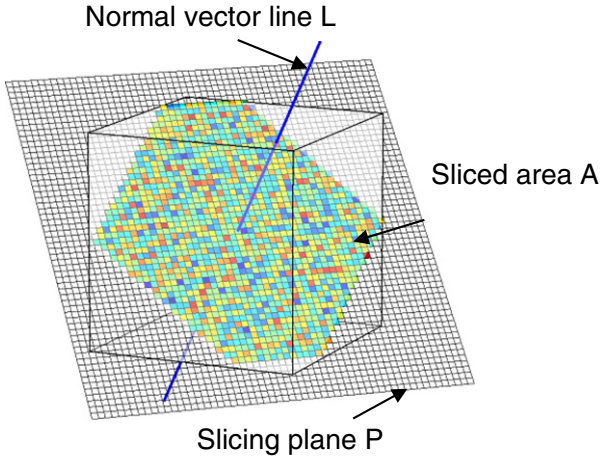

Fig. 1. Schematic illustration of the proposed concept. The slicing plane with a given orientation moves sequentially along the corresponding normal vector line L. The mean and standard deviation of the sliced voxels are obtained for all possible sets of trend and plunge of L.

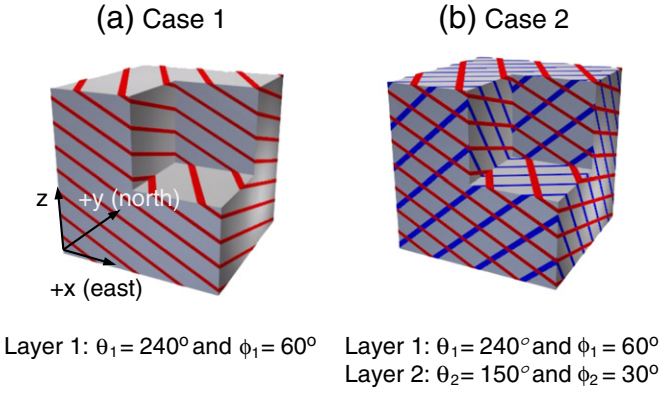

Fig. 2. 3D virtual structures with laminated layers. (a) Single-layered anisotropy, (b) double-layered anisotropy. θ and ϕ denote the trend and plunge of the normal vector of each slicing plane, respectively.